NON-SEPARABLE NON-LINEAR DECOMPOSITIONS WITH APPLICATIONS TO IMAGE COMPRESSION

Eduardo S. Cardoso Jr. *Eduardo A. B. da Silva*

PEE/COPPE/DEL/EE
Universidade Federal do Rio de Janeiro
Cx. P. 68504, Rio de Janeiro, RJ
21945-970, BRAZIL
xaua@lps.ufrj.br eduardo@lps.ufrj.br

Abstract

Linear separable multi-resolution decompositions are extensively used in many signal processing applications. Recently, there has been a growing interest in both non-linear and non-separable decompositions, due to their increased flexibility when compared to either linear or separable ones. Of special interest is the case where the decompositions are both non-linear and non-separable. However, up to now, there are no general tools for the design of such decompositions. This work suggests an heuristic to design maximally-decimated non-separable non-linear decompositions. First, a particular case of a non-separable structure found in the literature are presented. Then non-linear operators suitable for use in that are listed. The design strategy is described and preliminary non-linear-non-separable designs are generated. The image coding performance of these decompositions is very close to the one achievable with the best known linear filter banks. This suggests that the proposed heuristic is an effective tool for the design of non-linear decompositions, which opens exciting research possibilities.

1. INTRODUCTION

Critically-decimated linear multi-resolution decompositions play an important role in many signal processing applications, and they have been extensively investigated [1]. Recently there has been some interest in critically decimated *non-linear* multi-resolution decomposition, both *separable* and *non-separable* [2, 3, 4]. Perfect reconstruction is a key property of linear multi-resolution decompositions and several structures suitable for separable non-linear decompositions were presented enjoying that property [5, 6]. In [3], general structures are presented, including a non-separable one. A general framework for the theoretical analysis and generalization of such decompositions is presented in [4]. Despite all those efforts, the problem of designing such decompositions has not yet been solved.

This work suggests an heuristic to design maximally-decimated non-separable non-linear decompositions based on the non-separable structure presented in [3]. First, some simplifications to that structure are presented. Then non-linear operators suitable for use in the structure are listed. The design strategy is described and preliminary non-linear non-separable designs are generated. Finally, the designed decompositions are then evaluated in an image encoding framework.

2. NON-SEPARABLE DECOMPOSITIONS

When compared to separable decompositions, non-separable ones are more flexible and allow one to obtain detail bands with more general properties. In this paper are investigated the design and implementation of non-separable decompositions using the structure in figure 1, where x, y, z and w are the polyphase components of the input image $f(m,n)$, corresponding to $f(2m,2n)$, $f(2m,2n+1)$, $f(2m+1,2n)$ and $f(2m+1,2n+1)$, respectively. The signals $\tilde{x}$, $\tilde{y}$, $\tilde{z}$ and $\tilde{w}$ are the four-band output. This structure is a particular case of the general structure presented in [3]. Decompositions of several stages can be accomplished just by cascading structures like the one in figure 1. Note that the operators $T^l_{ab}(\cdot)$ and $S^l_{ab}(\cdot)$ can be non-linear. Using the one stage analysis structure in figure 1, perfect reconstruction can be achieved by just reversing the order of operations and the signs of the operators in the synthesis operation.

One should note that if we restrict the operators in figure 1 to $T^1_{11} = T^1_{12} = T^1_{20} = T^1_{30} \equiv T$, $-T^1_{10} \equiv (T)^2$, $T^1_{21} \equiv 0$, $S^1_{11} = S^1_{12} = S^1_{20} = S^1_{30} \equiv S$, $-S^1_{10} \equiv (S)^2$ and $S^1_{21} \equiv 0$, then the structure becomes separable [7].

In the following development we consider that $T^l_{ab}(\cdot) = ct^l_{ab}\,\tilde{T}^l_{ab}(\cdot)$ and $S^l_{ab}(\cdot) = cs^l_{ab}\,\tilde{S}^l_{ab}(\cdot)$, where ct^l_{ab} and cs^l_{ab} are scalars and $\tilde{T}^l_{ab}(\cdot)$ and $\tilde{S}^l_{ab}(\cdot)$ are non-linear operators. The design of such decompositions consists of,

0-7803-6297-7/00/$10.00

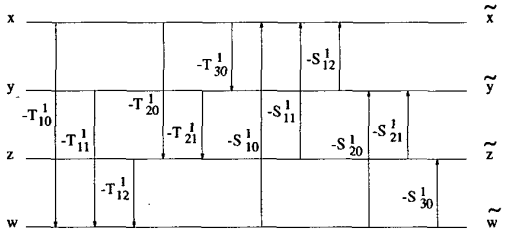

Fig. 1. Non-separable one stage decomposition.

given the operators $\tilde{T}_{ab}^l(\cdot)$ and $\tilde{S}_{ab}^l(\cdot)$, finding the ct_{ab}^l and cs_{ab}^l such that the resulting decompositions are "good" in some sense. For example, in several applications, one desires a four-band decomposition such as the one in figure 1 to generate a compact representation of the input signal. This in general leads to the output $\tilde{x}$ being an approximation band and the outputs $\tilde{y}$, $\tilde{z}$ and $\tilde{w}$ being bands with vertical, horizontal and diagonal details, respectively.

In that case, it is interesting that the non-linear operators used to implement the $\tilde{T}_{ab}^l(\cdot)$ and $\tilde{S}_{ab}^l(\cdot)$ satisfy general properties that make it easier to achieve the above mentioned goal.

These properties are as follows [8, 7]:

I. The operators should be smoothing functions, that is, they should generate a lower resolution approximation of the input;

II. They must not add a DC level to its input.

Although many non-linear operators enjoy property I, (for example, *median*, *opening* and *closing*), most of them do not enjoy property II (see that the morphological gray scale opening, $f \circ k$, has the property $f \circ k \leq f$ and the closing, $f \bullet k$, has the property $f \bullet k \geq f$ [9]). Two non-linear operators that enjoy both properties are as follows [8]:

$$\mathcal{L}_k(f) = \frac{(f \circ k) + (f \bullet k)}{2} \tag{1}$$

$$\mathcal{G}_k(f) = \frac{[(f \circ k) \bullet k] + [(f \bullet k) \circ k]}{2} \tag{2}$$

In order to obtain a useful decomposition, one must implement the operators $\tilde{T}_{ab}^l(\cdot)$ and $\tilde{S}_{ab}^l(\cdot)$ taking into account the relative sample positions of its input and output as explained below. The key concept is that each output of the operators $\tilde{T}_{ab}^l(\cdot)$ and $\tilde{S}_{ab}^l(\cdot)$ must be in the same sample positions with respect to the signal to which it will be added [7]. For example, referring to figure 1, the $\tilde{T}_{10}^1(\cdot)$ operator performs a modification of x and the negative of its output is multiplied by ct_{10}^1 and added to w. A way to implement this is to first create an interpolated image I having the samples x as its first polyphase component and η, the neutral element for the operator, as the other three. Then either the operator $\mathcal{L}_k(\cdot)$ or $\mathcal{G}_k(\cdot)$ is applied to I generating $\hat{I}$. The output of $\tilde{T}_{10}^1(\cdot)$ is the image obtained by sampling $\hat{I}$ in the same sample positions of the w polyphase component. This can be easily generalized for the other operators in the structure [7].

Note that, although the above procedure is not necessary for perfect reconstruction, we have verified experimentally that, in the non-linear case, severe quantization artifacts arise in case it is not carried out.

The neutral element η depends on the operation to be performed. In the linear case, $\eta = 0$. For the morphological gray-scale opening, $\eta = +\infty$, and for the morphological gray-scale closing, $\eta = -\infty$ [8, 7].

3. DESIGN OF THE DECOMPOSITION

In order to design "good" decompositions we have chosen to specify their behavior for four basic images with constant polyphase components: L is a constant image having $x = y = z = w = 1$ in all positions; H has horizontal details, that is, $x = y = 1$ and $z = w = -1$; V has vertical details, that is, with $x = z = 1$ and $y = w = -1$; and D has diagonal details, that is, $x = w = 1$ and $y = z = -1$.

The output equations are written for the four basic images and the restrictions below are applied yielding a system to be solved for the ct_{ab}^l and cs_{ab}^l. The restrictions were developed based on desirable directional properties. They are:

$$\begin{array}{llll} \tilde{x}^L = A_0 & \tilde{x}^H = 0 & \tilde{x}^V = 0 & \tilde{x}^D = 0 \\ \tilde{y}^L = 0 & \tilde{y}^H = 0 & \tilde{y}^V = A_2 & \tilde{y}^D = 0 \\ \tilde{z}^L = 0 & \tilde{z}^H = A_1 & \tilde{z}^V = 0 & \tilde{z}^D = 0 \\ \tilde{w}^L = 0 & \tilde{w}^H = 0 & \tilde{w}^V = 0 & \tilde{w}^D = A_3 \end{array} \tag{3}$$

where the superscript denotes the input image, and A_i denotes the desired gain for each band. For example, the above eqs. imply that, if the horizontal image H is input, the horizontal band has constant value equal to A_1 and the remaining ones are zero.

The equations can be written by taking into consideration the behavior of the operators as follows: the operators $\tilde{T}_{ab}^l(\cdot)$ and $\tilde{S}_{ab}^l(\cdot)$, when implemented as described in section 2 and using $\mathcal{L}_k(\cdot)$ or $\mathcal{G}_k(\cdot)$, behave like the identity for images with constant polyphase components, provided that a suitable structuring element k is used. A good choice is an element with symmetry around an extreme value and the axis of symmetry is located at a 1/2 sample position on the two axes of the two-dimensional grid [7]. Using the geometrical interpretations of the morphological opening and closing, we see that, with this symmetry, the umbra of k will never fit "inside" the holes represented by the neutral elements η in the interpolated image $\hat{I}$ (see figure 2 for an example in one-dimension). This implies that the interpolation positions are filled with the value of a neighboring sample, which in the case of the images L, H, V and D is

constant over the whole image[1].

This yields simplified non-linear equations with only multiplicative and additive combinations of ct^l_{ab} and cs^l_{ab}. The equations are too big to be included here, but can be found in [7]. Note that these equations hold for either $\mathcal{L}_k(\cdot)$ or $\mathcal{G}_k(\cdot)$.

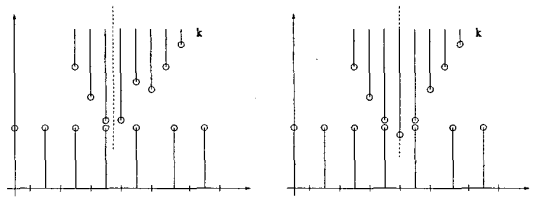

Fig. 2. Geometrical interpretation of the closing of a constant sequence: (a) k with desirable symmetry (b) k without desirable symmetry.

One important point in the design of such decompositions has to do with the structuring element k used in the morphological operations in the $\mathcal{L}_k(\cdot)$ and $\mathcal{G}_k(\cdot)$ operators. It can be shown that in the proposed structure, it is not possible to construct an horizontal band using a two-dimensional structuring element [7]. In order to construct the horizontal band $\tilde{z}$, the structuring elements of the transformations contributing to it must be unidimensional and have horizontal orientation. This is so because a morphological operation with such an element will not modify the vertical edges. As a consequence, the vertical edges in the polyphase component z will be canceled, yielding a band $\tilde{z}$ without vertical edges (see fig. 1). Analogous considerations can be made for the vertical band $\tilde{y}$. Thus, three structuring elements will be used in the implementation of $\mathcal{L}_k(\cdot)$ or $\mathcal{G}_k(\cdot)$: one two-dimensional k_b, one horizontal unidimensional k_h and one vertical unidimensional k_v. The operators $T^l_{10}(\cdot)$ and $S^l_{10}(\cdot)$ use k_b, the operators $T^l_{11}(\cdot)$, $T^l_{20}(\cdot)$, $S^l_{11}(\cdot)$ and $S^l_{20}(\cdot)$ use k_v and the operators $T^l_{12}(\cdot)$, $T^l_{30}(\cdot)$, $S^l_{12}(\cdot)$ and $S^l_{30}(\cdot)$ use k_h. The structuring element employed in the simulations was a parabola with dimensions 4x4 for k_b, 4x1 for k_v and 1x4 for k_h.

Experimental results have suggested that the design strategy presented leads to good non-linear decompositions, see table 1. Also, this strategy has generated non-separable decompositions having sub-bands with directional properties equivalent to the ones obtained with linear filter banks.

[1]It is important to note that for symmetry around an integer sample position, the operator will not have this behavior. Therefore, the equations would be dependent on the structuring element k, and will not have a closed algebraic form.

Filter	Gm2222	Lm2222	Gm1224	9-7
PSNR(dB)	29.56	29.74	26.11	31.01

Table 1. PSNR values for the studied decompositions.

	for $A_0 = 1, A_1 = -2,$ $A_2 = -2$ and $A_3 = 4$		for $A_0 = A_3 = 2$ and $A_1 = A_2 = -2$	
coefs.	$l = 1$	$l = 2$	$l = 1$	$l = 2$
ct^l_{10}	-0.165	-0.472	-0.212	-0.166
ct^l_{11}	0.650	0.374	0.168	0.514
ct^l_{12}	0.650	0.374	0.168	0.514
ct^l_{20}	0.520	0.449	0.274	0.588
ct^l_{21}	0.000	0.000	0.000	0.000
ct^l_{30}	0.520	0.449	0.274	0.588
cs^l_{10}	-0.369	0.162	-0.167	-0.212
cs^l_{11}	-0.052	-0.319	-0.588	-0.274
cs^l_{12}	-0.052	-0.319	-0.588	-0.274
cs^l_{20}	-0.232	-0.433	-0.514	-0.168
cs^l_{21}	0.000	0.000	0.000	0.000
cs^l_{30}	-0.232	-0.433	-0.514	-0.168

Table 2. Coefficients of the designed decompositions.

4. EXPERIMENTAL RESULTS

In this section, we present two non-separable non-linear decompositions designed using the method presented in section 3. The output equations with the restrictions in eq. 3 and the considerations in sections 2 and 3 yield a non-linear system of equations that can be solved using numerical techniques. In order to simplify the solution of the equations we have assumed that $T^l_{21}(\cdot) = 0$ and $S^l_{21}(\cdot) = 0$. The decompositions designed are two-stage, that is, we have cascaded two structures having the form as in figure 1. It is important to point out that for one stage the equations have no solution.

One decomposition was designed for $A_0 = A_3 = 2$, $A_1 = A_2 = -2$, and another for $A_0 = 1$, $A_1 = A_2 = -2$, $A_3 = 4$ (see eq. 3). We refer to these decompositions as *Gm2222*, *Lm2222* and *Gm1224*. The numbers refer to the values of $A_0 \ldots A_3$ and, G to the operator $\mathcal{G}_k(\cdot)$ and L to the operator $\mathcal{L}_k(\cdot)$. The coefficients are shown in table 2 (rounded to 3 significant digits).

For comparison purposes we have employed the above non-linear decompositions in order to generate a non-separable two-dimensional 5-stage octave-band decomposition. Such decomposition was used to replace the wavelet transform stage in the EZW coder [10]. The PSNR results for the Lena 521x512 image using a bit-rate of 0.15 bpp are summarized in table 1, along with results for the Daubechies 9-7 filter bank [11].

The reconstructed images for the *Gm2222* and *Lm2222* decompositions presented have shown a subjective quality comparable to the one of the linear 9-7 wavelet. One example can be seen in figure 3. With a careful examination, we can see that the non-separable non-linear decomposition generates a little less ringing artifacts, while presenting a slight increase in blockness.

It is interesting to note that, if the operators $\mathcal{L}_k(\cdot)$ and $\mathcal{G}_k(\cdot)$ were linear, the gains $A_0 = A_3 = 2$ and $A_1 = A_2 = -2$ would yield a decomposition with $H_0(z_1, z_2)G_0(z_1, z_2)|_{z_1=1, z_2=1} = \sqrt{2}$ [1], that is essential in order for the decomposition to be a wavelet transform. This is not the case for the gains $A_0 = 1$, $A_1 = -2$, $A_2 = -2$ and $A_3 = 4$, and in fact the reconstructed image has a PSNR 2.5dB lower then the *Gm2222* case.

An important point is that both *Gm2222* and *Gm1224* decompositions satisfy the design constraints (see eq. 3). The fact that the first has a better performance indicates that further research must be carried out in order to find criteria to generate optimum decompositions. However, the method presented here is sufficient to generate good decompositions and is thus a valuable tool in the search for more effective design methods.

Fig. 3. Lena 512x512 at 0.15 bpp for Gm2222.

5. CONCLUSION

In this paper we introduced a heuristic approach to the problem of designing non-separable non-linear decompositions. Three decompositions were designed, and then tested in the framework of an EZW coder, generating reconstructed images with a subjective quality comparable to the best linear ones in the literature. However, an important point is that these heuristics leave many degrees of freedom as the number of stages and the values of the A_j in eq. 3. Therefore, we still need criteria for finding the best among such solutions. Nevertheless, considering the flexibility provided by non-linear decompositions, this heuristic is a powerful tool for designing alternative signal decompositions.

It is important to note that the design of non-separable non-linear maximally decimated decompositions is still an open problem. However, we believe that, although we have presented just a heuristic approach to such design, its strength lies on the fact that it opens new venues in the direction of finding more effective design methods.

6. REFERENCES

[1] P. P. Vaidyanathan, *Multirate Systems and Filter Banks*. Englewood Cliffs, NJ: Prentice-Hall, 1993.

[2] D. Taubman, "Adaptive, non-separable lifting transforms for image compression," in *1999 IEEE International Conference on Image Processing*, 1999.

[3] F. J. Hampson and J.-C. Pesquet, "M-band nonlinear subband decompositions with perfect reconstruction," *IEEE Transactions on Image Processing*, vol. 7, pp. 1547–1560, November 1998.

[4] J. Goutsias and H. J. A. M. Heijmans, "Multiresolution signal decompositions schemes. part 2: Morphological wavelets.," Technical Report PNA-R9905, CWI, Amsterdam, The Netherlands, June 1999.

[5] O. Egger, W. Li, and M. Kunt, "High compression image coding using an adaptive morphological subband decomposition," in *Proceedings of IEEE*, vol. 83, pp. 272–287, 1995.

[6] D. A. F. Florêncio and R. W. Schafer, "Perfect reconstructing nonlinear filter banks," in *Proceedings of the 1996 ICASSP Conference*, vol. III, pp. 1815–1818, 1996.

[7] E. S. Cardoso, "Compressão de imagens utilizando decomposições em multiresolução morfológicas," Master's thesis, Federal University of Rio de Janeiro, Rio de Janeiro, Brazil, March 1999. URL http://www.lps.ufrj.br/projects/proj20.html.

[8] E. S. Cardoso and E. A. B. da Silva, "Design of nonlinear multi-resolution decomposition schemes using morphological operations," *Electronics Letters*, vol. 36, pp. 843–845, 27th April 2000.

[9] R. M. Haralick and L. G. Shapiro, *Computer and Robot Vision*. Addison-Wesley Publishing Company, 1992.

[10] J. M. Shapiro, "Embedded image coding using zerotrees of wavelet coefficients," *IEEE Transactions on Acoustics, Speech and Signal Processing*, vol. 41, pp. 3445–3462, December 1993.

[11] M. Antonini, M. Barlaud, P. Mathieu, and I. Daubechies, "Image coding using wavelet transform," *IEEE Transactions on Image Processing*, vol. 1, pp. 205–220, April 1992.